HFCC3
سومین کنفرانس هیدروژن و پیل سوختی
3rd Hydrogen & Fuel Cell Conference
Iranian Research Organization for Science & Technology (IROST)
IHFCA
Iranian Hydrogen & Fuel Cell Association (IHFCA)
IREIC
Fuel Cell Steering Committee

Modeling of Two-Phase flow in the Cathode Gas Diffusion Layer to Investigate Its Effects on a PEM Fuel Cell

Navid Aminnia
MSc Student, Department of Energy Systems, K. N. Toosi University of Technology
Majid Shateri
PhD Student, Department of Energy Systems, K. N. Toosi University of Technology
Sepideh Gheibi
MSc, Department of Energy Systems, K. N. Toosi University of Technology
Farschad Torabi*
Assistant Professor., Department of Energy Systems, K. N. Toosi University of Technology, ftorabi@kntu.ac.ir

Abstract Polymer Exchange Membrane (PEM) fuel cells are known as the most significant alternatives to internal-combustion engines, but still there is a long way to achieve this ideal in reality. To achieve such a goal lots of optimizations are needed to be done on fuel cells. Water management is critical for achieving high performance of PEM fuel cells. In high-current densities, condensed water fills the pores of the Gas Diffusion Layers and thus oxygen transfer to the catalyst layers would be limited. In this study, for the sake of analyzing the PEM fuel cell characteristics and their variations, using the COMSOL software, the two-phase flow regime in PEM fuel cells was simulated. To determine the saturation level in the cathode, a separate differential equation for mass conservation of liquid water was solved and due to the dependencies of other parameters of the mixture on the saturation level, these parameters are determined.

Keywords: PEM Fuel Cell, Fuel Cell modeling, Two-Phase flow

1. Introduction

Hydrogen is the major choice considered as the new energy carrier. This substance, compared to other fuels, can be transformed to other forms of energy with greater efficiency and a highly cleaner combustion. Abundance, unique applications, considerably small greenhouse effects, negligible pollutant emission and the reversible cycle of its formation are among the features that distinguish hydrogen from other fuel choices. Today, applications of fuel cells promise a bright future. Fuel cell applications include a wide range from space crafts to supplying energy for small electronic apparatus.

Experiments are the most common method of research in the field of fuel cells. In order to conduct any experiment, it is necessary to be in a completely controlled condition and study a specific parameter. It is usually a time-consuming process. On the other hand, it is possible to reach a profound

comprehension of fuel cells and related processes, utilizing mathematical modeling, which in return, reduces the needed experiments greatly. Mathematical modeling Not only makes us capable of predicting the fuel cells' behavior under various operation conditions and different design parameters, also makes the optimization of fuel cells less expensive and time consuming.

Extensive researches have been carried out to simulate the fuel cells' behavior. For instance, Bernardi and Verbrugge [1, 2] and Springer et al. [3, 4] built one-dimensional models. Fuller and Newman [5], Nguyen and White [6] and Gurau et al. [7] presented pseudo two-dimensional models that were actually the models along the fluid path. In all mentioned models, a certain system of equations was presented for each region of the cell, so boundary conditions were required for combining all the regions and obtaining a consistent solution for all the regions.

Water management issue is one of the most important aspects of numerical modeling efforts. In this regard, the pioneer Bernardi [9] analyzed the effect of different operating conditions on water balance in fuel cells. Wang and Savinell [10] studied the effect of electrode structure on water transportation in the catalyst layer. Fuller and Newman [6] simulated the fuel cell performance with humidified input gases by implementing a virtual two-dimensional model for the membrane and electrode regions. They determined the water distribution in the membrane and its net passing water flow. Nguyen and White [7] compared three humidification schemes by combining mass and heat transfer models. Springer et al. [5] predicted the ratio of water flow to proton flow in the membrane. In the latter work, Springer et al. compared the predicted results with experimental data. By just correcting the effective porosity for the transportation of oxygen in the presence of water, Bernardi and Verbrugge [1, 2] formulated the simplified one-dimensional model for liquid water transportation. Wang et al. [8] simulated cathode operation in the two-phase multicomponent mixture region, by applying a model in conjunction with a finite-volume-based computational fluid dynamics (CFD) technique. In the present study, it was predicted that liquid water saturation in the current density of 1.4 $A.cm^{-2}$ reaches up to 6.3 percent.

Khakbaz and Kermani [9] studied a two-dimensional, isothermal and two-phase model to simulate the two-phase flow in fuel cells. Khakbaz and Kermani did not model the fuel cell completely. Their computational space includes the channel and the porous gas diffusion layer, therefore the law of electrical charge conservation was not considered in this model. Furthermore the catalyst region was considered as an infinitely thin layer and amount of produced water as a result of electrochemical reactions in constant density was implemented as a boundary condition in this layer.

In order to complete the model developed by Khakbaz and Kermani and achieve a more realistic model, in the present research, a single cell fuel cell is modeled completely and all the fuel cell regions are modeled with actual dimensions. The conservation law of electrical charge is applied to anode and cathode gas diffusion and catalyst layers and also polymer membrane. As a result, the current density distribution is attained. Having the current density distribution, the boundary conditions of liquid water mass conservation equation at the interface between gas diffusion and catalyst layers are applied with

more accuracy and the saturation level would be corrected.

2. Governing Equation

Microscopic Conservation Equations in Single-Phase Flow

In multi-phase electrochemical systems, as in porous electrodes, electrochemical processes are generally stated by the conservation laws of mass, momentum, chemical species and electrical charge at each phase. In most porous electrodes, there is no fluid movement or it can be neglected. As a result the mass and momentum equations will be removed from the system of equations. But, in the model presented in this research, in order to generalize the formula, these equations are considered, too.

Momentum and mass conservation law

The fluid motion in phase *k* can be stated by conservation laws of mass and momentum. These laws are described below. Principle of conservation of mass [10]:

$$\frac{\partial(\rho\varepsilon)}{\partial t} + \nabla.(\varepsilon\rho\overrightarrow{v}) = 0 \qquad (1)$$

Porosity coefficient is added to the equation of mass conservation due to existence of the porous media in the fuel cell. In the above equation ρ is density, v is the scalar velocity, and ε is the porosity coefficient.

Principle of momentum conservation [10]:

$$\frac{\partial(\rho\varepsilon)}{\partial t} + \nabla.(\varepsilon\rho\vec{v}\vec{v}) = -\varepsilon\nabla p + \nabla.\left(\varepsilon\mu^{\text{eff}}\nabla v\right) + S_u \qquad (2)$$

Similar to the previous equation, porosity coefficient is added to this equation due to the existence of porous media in the fuel cell. S_u is related to source of the equation and takes different values in different regions of the cell. S_u in the gas diffusion layer is as follows:

$$S_u = -\frac{\mu}{K}\varepsilon^2 u \qquad (3)$$

where μ is fluid viscosity, K is the diffusion resistance at the gas diffusion layer, ε is the porosity of the layer and u is the fluid velocity. In the catalyst layer we have:

$$S_u = -\frac{\mu}{K_p}\varepsilon_m\varepsilon_{mc}u + \frac{k_\phi}{k_p}z_f c_f F\nabla\Phi_e \quad (4)$$

where k_p is the hydraulic resistance of the membrane. ε_{mc} and ε_m are porosity of the catalyst layer and membrane in the catalyst region respectively. k_ϕ is electro kinetic diffusion resistance. c_f and z_f and F are concentration, charge number, and Faraday number, respectively.

Finally, the momentum in the polymer membrane layer of the sink is as follows:

$$S_u = -\frac{\mu}{K}\varepsilon_m u + \frac{k_\phi}{k_p}z_f c_f \nabla\Phi_e \quad (5)$$

Principle of conservation of chemical species

Mass balance for species in phase *k* is:

$$\frac{\partial(\varepsilon X_k)}{\partial t} + \nabla.(\varepsilon v X_k) = \nabla.\left(D_k^{\text{eff}}\nabla X_k\right) + S_k \quad (6)$$

where X_k is the species, S_k is the sink or source of the species and D_k is the diffusion coefficient of the species. Since the species exist in a porous media, the amount of diffusion coefficient differs from the physical diffusion coefficient of a pure material and it is necessary to obtain its effective amount using Bruggman equation [11]:

$$D_k^{\text{eff}} = \varepsilon^{1.5}D_k \quad (7)$$

where is D_k the diffusion coefficient of pure material that is a function of temperature. This value can be functionally calculated as follows:

$$D_k(T) = D_0(\frac{T}{T_0})(\frac{P_0}{P}) \quad (8)$$

where D_0 is equal to the diffusion coefficient of the species at reference condition of temperature and pressure (T=273.15°C and P=1 atm).

The source term, S_k is defined as:

$$S_k = \pm \frac{J}{aFc_{tot}} \quad (9)$$

where J is the production source of electrical ions and c_{tot} is the total amount of reactant entering the main channel that intended species constitutes a fraction of it. a is a coefficient that is variable considering the material and its location.

Conservation of electrical charge

Electrochemical reactions happen in the interface between active material and electrolyte; therefore no charge is created in phase k nor consumed. This principle which is known as electroneutrality states that net flow input onto a phase is equal to net flow output from that phase, so:

$$\nabla.\vec{i}_k = 0 \quad (10)$$

But flow generated on boundaries enters the phases, so the boundary condition for each phase is as follows:

$$\vec{i}_k.\vec{n}_k = -\sum_j i_{nj} \quad (11)$$

In these equations, $\vec{i}_k$ is current density in phase k. This electrical current is carried by electrons in solid materials, and its governing equation is explained by Ohm principle as follows:

$$\vec{i}_s = -\sigma \nabla \phi_s \quad (12)$$

In this equation, $\vec{i}_s$ and ϕ_s are current and potential in solid electrode, respectively and σ is its electrical conductivity. Either in solid or in liquid phase, the charge transfer is accomplished by ions movement which happens in three ways as follows:

a. Ions diffusion that happens due to the existence of ions and is stated by Fick's law.
b. Electrolyte movement that, as noted before, is accomplished in liquid electrolytes.
c. Migration that is accomplished due to the existence of electrical potential gradient in battery.

In electrolyte phase, a proper form of Ohm's law should be used which consists of both effects of concentration and potential gradient. This principle is known as modified Ohm's law which can be described as follows:

$$\vec{i}_e = -k\nabla\phi_e - k_D\nabla\left(ln\, c_e^i\right) \qquad i = \pm \quad (13)$$

where k is effective conductivity of electrolyte and k_D is diffusion conductivity which exists to consider

the effect of ions movement and diffusion in presence of concentration gradient. The symbols + and − are positive and negative poles, respectively. Now, if the effects of conservation gradient are ignored, the equation of conservation of electrical charge is:

$$\nabla.\left(\sigma_e^{\text{eff}}\nabla\Phi_e\right) + S_\Phi = 0 \qquad (14)$$

where σ_e^{eff} is the effective conductivity of solid membrane phase which is modified by Bruggman equation as follows:

$$\sigma_e^{\text{eff}} = \varepsilon^{1.5}\sigma_e \qquad (15)$$

In this equation ε is porosity coefficient and σ_e is a function of temperature [10]. The source of ion production in equation (14) is calculated as follows:

$$S_\phi = J \qquad (16)$$

where J is calculated using electrochemical reactions on the sides of anode and cathode respectively as follows:

$$J_a = aj_{0_a}^{\text{ref}}\left(\frac{X_{H_2}}{X_{H_{2,\text{ref}}}}\right)^{0.5}\left(\frac{\alpha_a + a_c}{RT}.F.\eta\right) \qquad (17)$$

$$J_c = -aj_{0_c}^{\text{ref}}\left(\frac{X_{O_2}}{X_{O_{2,\text{ref}}}}\right)^{0.5}\exp\left(-\frac{a_c F}{RT}.\eta\right) \qquad (18)$$

In these two equations $aj_{0_a}^{\text{ref}}$ and $aj_{0_c}^{\text{ref}}$ are the amount of reference electrical current multiplied by the active area of the anode and cathode, respectively. Also α_a and α_c are the charge transfer coefficient of anode and cathode, respectively. In these two equations, η is the overpotential which is described as follows:

$$\eta = \Phi_s - \Phi_e - V_{oc} \qquad (19)$$

where Φ_s is solid phase voltage, Φ_e is electrolyte voltage and V_{oc} is open circuit voltage.

Microscopic conservation equations in two-phase flow

When the cell is operating at a current density higher than the critical current density, liquid water will appear and two-phase flow occurs at the cathode. Polymer membrane, as a proton source, is in need of sufficient water for high ion conduction. In a fuel cell, water molecules use electro-osmotic

drag force for transporting. Because of fluid convection and molecular diffusion, maintaining water content in polymer membrane is difficult, so the reactants are humidified at the anode or cathode inlet. On the other hand, water is produced at the interface between the cathode and membrane as a result of electrochemical reaction between H^+ and O_2. If water is not removed from cathode with a suitable rate, water may be accumulated at the cathode and oxygen transport to the reaction site may be deferred. Therefore some amount of dry air is necessary to exist at the cathode inlet in order to remove surplus water [12].

Governing differential equations are:

- Conservation equation of species for oxygen, hydrogen and water
- Momentum equation for the mixture of oxygen and hydrogen
- Mass conservation equation of liquid phase
- Mass conservation equation of mixture of gases

In this study, the mixture at cathode consists of oxygen, nitrogen, liquid water and water vapor and at the anode it consists of hydrogen and water vapor. Continuity equation for the two-phase mixture (gas and liquid) is as follows:

$$\frac{\partial(\epsilon\rho)}{\partial t} + \nabla.\left(\epsilon\rho\vec{V}\right) = 0 \qquad (20)$$

where ϵ is the porosity for the gas diffusion layer; ρ is the density of the two-phase mixture and $\vec{V}$ is the mass mean velocity of the mixture. The saturation level in the fuel cell can be predicted by the following equation:

$$\frac{\partial(\epsilon s\rho_l)}{\partial t} + \nabla.\left(\epsilon s\rho_l\vec{V_l}\right) = \epsilon\dot{S}_l \qquad (21)$$

This is the continuity equation for water and ρ_l is the liquid phase density; s is the saturation level and $\vec{V_l}$ is the liquid phase velocity; $\dot{S}_l$ is the condensation rate per unit volume and is calculated by the following equation:

$$\dot{S}_l = -\frac{1}{R_{H_2O}}\left[P_{sat}\left(\frac{1-s}{T}\right)^{t+\Delta t} - P_{H_2O}\left(\frac{1-s}{T}\right)^{t}\right] \qquad (22)$$

In this equation P_{H_2O} is the partial pressure before condensation and P_{sat} is the water vapor saturation pressure after the condensation. There is thermodynamic instability in the first case and stability in the latter case at the two-phase region. R_{H_2O} is the water vapor gas constant. Mass balance for water vapor is

as follows:

$$\frac{\partial(\epsilon(1-s)\rho_g C_g^{H_2O})}{\partial t} + \nabla.\left(\epsilon(1-s)\vec{N}_{H_2O}\right) = \epsilon\dot{S}_g \quad (23)$$

$C_g^{H_2O}$ is vapor concentration and is calculated by the following equation:

$$C_g^{H_2O} = \frac{\rho_g^{H_2O}}{\rho_g} \quad (24)$$

In this equation ρ_g is the gas phase density and $\rho_g^{H_2O}$ is water vapor density; $\dot{S}_g$ is the rate of water vaporization and is calculated as follows:

$$\vec{S}_g = -\vec{S}_l \quad (25)$$

$\vec{N}_{H_2O}$ in the equation (23) is water vapor mass flow rate and is calculated by the following equation:

$$\vec{N}_{H_2O} = \rho_{H_2O}\vec{V}_g + \vec{J}_{H_2O} \quad (26)$$

In this equation $\vec{V}_g$ is the mass mean velocity of the gas phase and calculated by the equation (42). $\vec{J}_{H_2O}$ is mass diffusion flow rate of water vapor that can be calculated by the Stefan-Maxwell equation [12]. Mass diffusion flow rates for two-component mixture are determined by the Fick's law. An appropriate model for multi-component diffusion is the Stefan-Maxwell model.

If the mixture is assumed as ideal gas, density may be calculated by the following equation [13]:

$$\rho = CRT \quad (27)$$

C is the solution concentration and is calculated by the following equation:

$$C = \frac{[\rho + (M_3 - M_1)C_1 + (M_3 - M_2)C_2]}{M_3} \quad (28)$$

Diffusion flow rates are calculated by Stefan-Maxwell equation [13]:

$$\begin{bmatrix}\vec{J}_1^* \\ \vec{J}_2^*\end{bmatrix} = \begin{bmatrix}D_{11} & D_{12} \\ D_{21} & D_{22}\end{bmatrix}\begin{bmatrix}\nabla\left(\frac{C_1}{C}\right) \\ \nabla\left(\frac{C_2}{C}\right)\end{bmatrix} \quad (29)$$

In this equation *D* is the Stefan-Maxwell matrix. Each component of this matrix is related to the binary diffusion and is calculated by one of the following equations:

$$D_{11} = \frac{\Delta_{13}\left(\left(\frac{C_1}{C}\right)\Delta_{23} + \left(1-\frac{C_1}{C}\right)\Delta_{12}\right)}{S}$$

$$D_{12} = \frac{\frac{C_1}{C}\Delta_{23}(\Delta_{13}-\Delta_{12})}{S} \quad (30)$$

$$D_{21} = \frac{\frac{C_2}{C}\Delta_{13}(\Delta_{23}-\Delta_{12})}{S}$$

$$D_{22} = \frac{\Delta_{23}\left(\frac{C_2}{C}\Delta_{13} + \left(1-\frac{C_2}{C}\right)\Delta_{12}\right)}{S}$$

In these equations, Δ_{12}, Δ_{13}, and Δ_{23} are binary diffusions. *S* in these equations is calculated by the following equation:

$$S = \frac{C_1}{C}\Delta_{23} + \frac{C_2}{C}\Delta_{13} + \frac{C_3}{C}\Delta_{12} \quad (31)$$

Mole and mass diffusion flow rates are related by the following equations:

$$\begin{bmatrix}\vec{J}_1 \\ \vec{J}_2\end{bmatrix} = \begin{bmatrix}S_{11} & S_{12} \\ S_{21} & S_{22}\end{bmatrix}\begin{bmatrix}\vec{J}_1^* \\ \vec{J}_2^*\end{bmatrix} \quad (32)$$

In this equation the components of the conversation matrix *S* are calculated by the following relations:

$$s_{kl} = \delta_{kl} - \frac{C_k M_l}{\rho}\left(1-\frac{M_3}{M_1}\right) \qquad k,l = 1,2 \quad (33)$$

$$\begin{cases}\delta_{kl}=1 & k=1\\ \delta_{kl}=0 & k\neq 1\end{cases} \tag{34}$$

By combining equations (29) and (32) the following equation is achieved:

$$\begin{bmatrix}\vec{j}_1\\ \vec{j}_2\end{bmatrix}=-\begin{bmatrix}a & b\\ c & d\end{bmatrix}\begin{bmatrix}\nabla\left(\frac{C_1}{C}\right)\\ \nabla\left(\frac{C_2}{C}\right)\end{bmatrix} \tag{35}$$

The values *a*, *b*, *c* and *d* are calculated as follows:

$$\begin{aligned}a&=C[s_{11}D_{11}+s_{12}D_{21}]\\ b&=C[s_{11}D_{12}+s_{12}D_{22}]\\ c&=C[s_{21}D_{11}+s_{22}D_{21}]\\ d&=C[s_{21}D_{12}+s_{22}D_{22}]\end{aligned} \tag{36}$$

Mass balance for oxygen is determined as follows:

$$\frac{\partial(\epsilon(1-s)\rho_g C_g^{O_2})}{\partial t}+\nabla.\left(\epsilon(1-s)\vec{N}_{O_2}\right)=0 \tag{37}$$

In this equation $C_g^{O_2}$ is oxygen concentration and is calculated as follows:

$$C_g^{O_2}=\frac{\rho_g^{O_2}}{\rho_g} \tag{38}$$

$\vec{N}_{O_2}$ is the oxygen mass flow rate and is calculated as follows:

$$\vec{N}_{O_2}=\rho_{O_2}\vec{V}_g+\vec{J}_{O_2} \tag{39}$$

$\vec{J}_{O_2}$ is the diffusion mass flow rate for oxygen and is calculated by Stefan-Maxwell equation. Momentum equation of the two-phase mixture at the open channel and gas diffusion layer is indicated as follows:

$$\frac{\partial(\epsilon\rho\vec{V})}{\partial t}+\nabla.\left(\epsilon\rho\vec{V}\,\vec{V}\right)=-\epsilon\nabla P+\nabla\left(\epsilon\lambda\nabla.\vec{V}+\delta 2\epsilon\mu\nabla.\vec{V}\right)+\epsilon\rho_k\vec{g}-\frac{\epsilon^2\mu}{K}\vec{V} \tag{40}$$

where ρ is the mixture density, μ is the mixture viscosity, ρ_k is the kinetic density.in this equation λ is calculated by the following relation:

$$\lambda = -\frac{2}{3}\mu \tag{41}$$

Gas and liquid phase velocities are determined as follows:

$$\epsilon\rho_l\vec{V_l} = j_l + \epsilon\lambda_l\rho\vec{V}$$
$$\epsilon\rho_g\vec{V_g} = j_g + \epsilon\lambda_g\rho\vec{V} \tag{42}$$

In these equations j_l is liquid phase diffusion and j_g is gas phase diffusion. These are correlated by the following relation:

$$j_g = -j_l \tag{43}$$

j_l is calculated as follows:

$$j_l = \frac{\lambda_l\lambda_g K}{\nu}[\nabla P_c + (\rho_l - \rho_g)\vec{g}] \tag{44}$$

In this equation, ν is the kinetic viscosity and is calculated by the following relation:

$$\nu = \frac{\mu}{\rho} \tag{45}$$

λ is relative mobility that for the liquid and gas phase is calculated as follows:

$$\lambda_l = \frac{\frac{K_{rl}}{\upsilon_l}}{\frac{K_{rg}}{\upsilon_g} + \frac{K_{rl}}{\upsilon_l}} \tag{46}$$

$$\lambda_g = 1 - \lambda_l \tag{47}$$

K_{rl} and K_{rg} are relative diffusion of liquid and gas phase and are calculated by equation (53); υ_l and υ_g are kinetic viscosity of liquid and gas phase. In the equation (44) P_c is the capillary pressure for hydrophilic surface and is calculated as follows:

$$P_c = C[1.417(1-s) - 2.12(1-s)^2 + 1.263(1-s)^3] \quad (48)$$

By considering $\sigma_c = 0.067\ \mathrm{N\ m^{-1}}$ at the temperature 50°C and $\theta_c = 60°\mathrm{C}$ the value of C in the equation (48) is calculated by the following equation:

$$C = \sigma_c \cos\theta_c \left(\frac{\epsilon}{K}\right)^{\frac{1}{2}} \quad (49)$$

In order to determine gas density, ideal gas principle can be used. Mixture density (including both liquid and gas phases) is calculated as follows:

$$\rho = (1-s)\rho_g + s\rho_l \quad (50)$$

Kinetic density which appeared in the equation (40) is in order to take into account the acceleration of gravity at each phase and is calculated by the following equation:

$$\rho_k = \rho_g \lambda_g + \rho_l \lambda_l \quad (51)$$

The two-phase mixture viscosity is determined as follows:

$$\mu = \frac{\rho_l s + (1-s)\rho_g}{\frac{K_{rg}}{\nu_g} + \frac{K_{rl}}{\nu_l}} \quad (52)$$

In the viscosity equation, mass diffusion of phases is determined by experimental equations:

$$K_{rl} = s^3 \qquad K_{rg} = (1-s)^3 \quad (53)$$

3. Results

As shown in Figure 1, the considered fuel cell consists of oxygen and hydrogen channels shaped in a serpentine form. Since the cell performance along these channels is almost consistent, considering one part of the channel to simulate flow in the cell is sufficient. The considered model is consisted of seven parts as follows:

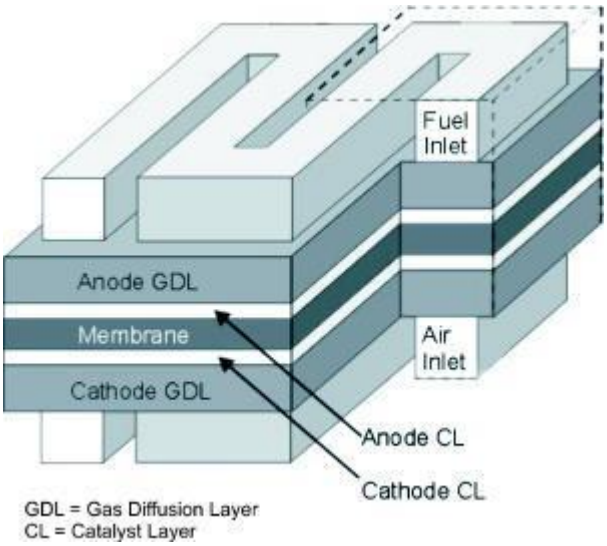

Figure 1. A complete package of a fuel cell [14]

1. Fuel (Hydrogen) Inlet Channel
2. Gas Diffusion Layer
3. Anode Catalyst Layer
4. Membrane
5. Cathode Catalyst Layer
6. Oxygen Diffusion Layer
7. Air (Oxygen) Inlet Channel

A general view of the geometry and mesh structure of the model is depicted in Figure 2. The physical and geometric characteristics of the model are also listed in Table 1.

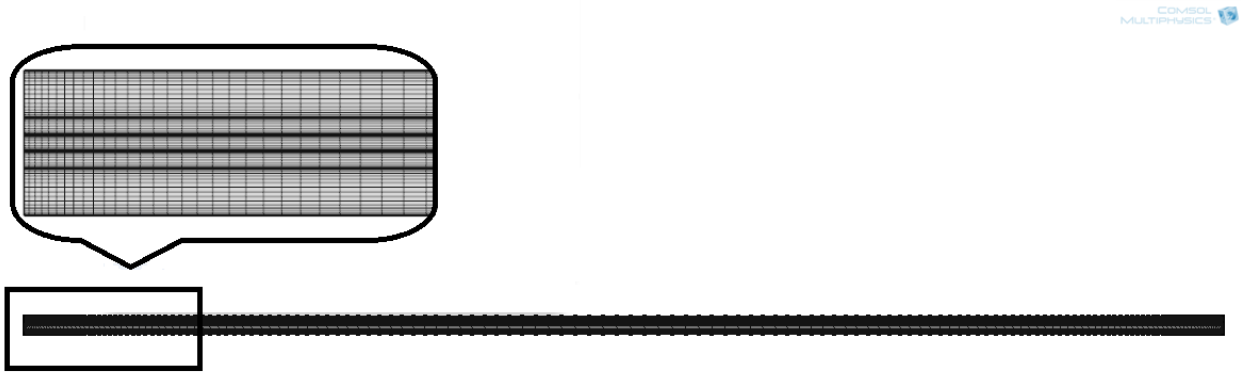

Figure 2. Geometry and Mesh Structure of the Model

Table 1. Model physical and geometrical characteristics

Parameter	Notation	Value	Reference
Cell Length	l_{cell}	7.112 cm	[10]
Air and Fuel Channel Width	w_{ac}, w_{fc}	0.0762 cm	[10]
Diffusion Layers Width	w_{GDL}	0.0254 cm	[10]
Catalyst Layers Width	w_{cl}	0.00287 cm	[10]
Polymer Membrane Width	w_m	0.023 cm	[10]
Diffusion Layers Porosity	ε	0.4	[10]
Catalyst Layers Porosity	ε_{cl}	0.4	[10]
Polymer Membrane Porosity	ε_m	0.28	[10]
Cell Temperature	T	50°C	[10]
Fuel Channel Pressure	P	3 atm	[10]
Air Channel Pressure	P	5 atm	[10]

Dual Diffusion Coefficient of Oxygen and Water	$D_{O_2-H_2O}$	5.6740×10^{-6} m^2s^{-1}	[10]
Dual Diffusion Coefficient of Water and Hydrogen	$D_{H_2O-H_2}$	2.8752×10^{-6} m^2s^{-1}	[10]
Dual Diffusion Coefficient of Nitrogen and Water	$D_{N_2-H_2O}$	2.7979×10^{-6} m^2s^{-1}	[10]
Dual Diffusion Coefficient of Oxygen and Nitrogen	$D_{O_2-N_2}$	2.6082×10^{-6} m^2s^{-1}	[10]
Cell Voltage	V	0.4 V	[10]
Backing Layers Permeability	K	1.76×10^{-11} m^2	[10]
Catalyst Layers Permeability	K_{cl}	7.18×10^{-16} m^2	[10]
Backing Layers Electric Conduction	σ_B	222 s m^{-1}	[10]
Ion Membrane Conduction	σ_m	9.825 s m^{-1}	[10]
Anode Transportation Coefficient	α_a	0.5	[12]
Cathode Transportation Coefficient	α_c	0.5	[12]
Anode Transfer Current Density	j_{oa}^{ref}	1×10^5 A m^{-2}	[10]
Cathode Transfer Current Density	j_{oc}^{ref}	1 A m^{-2}	[10]
Oxygen Reference Concentration	$C_{O_2}^{ref}$	17.817 mol m^{-3}	[10]
Hydrogen Reference Concentration	$C_{H_2}^{ref}$	66.817 mol m^{-3}	[10]
Specific Area of the Active Surface	A_v	1×10^4 m^{-1}	[10]

Polarization Curve and Model Validation

The polarization curve resulted from the presented simulation is shown in Figure 3. As it can be

seen in the figure, a good agreement has been attained between the results of the simulation and that one's published by Ticianely et al. [15]. As the figure shows, the maximum current density resulted from the model is equal to 0.72 $A.cm^{-2}$ in voltage of 0.15 V. Calculations show that for the fuel cell studied in this research, two-phase flow occurs at a current density about 0.1 $A.cm^{-2}$. The existence of two-phase flow in the pores of the backing layer delays the arrival of oxygen to the reaction site and accelerates the decreasing of the cell voltage in the polarization curve.

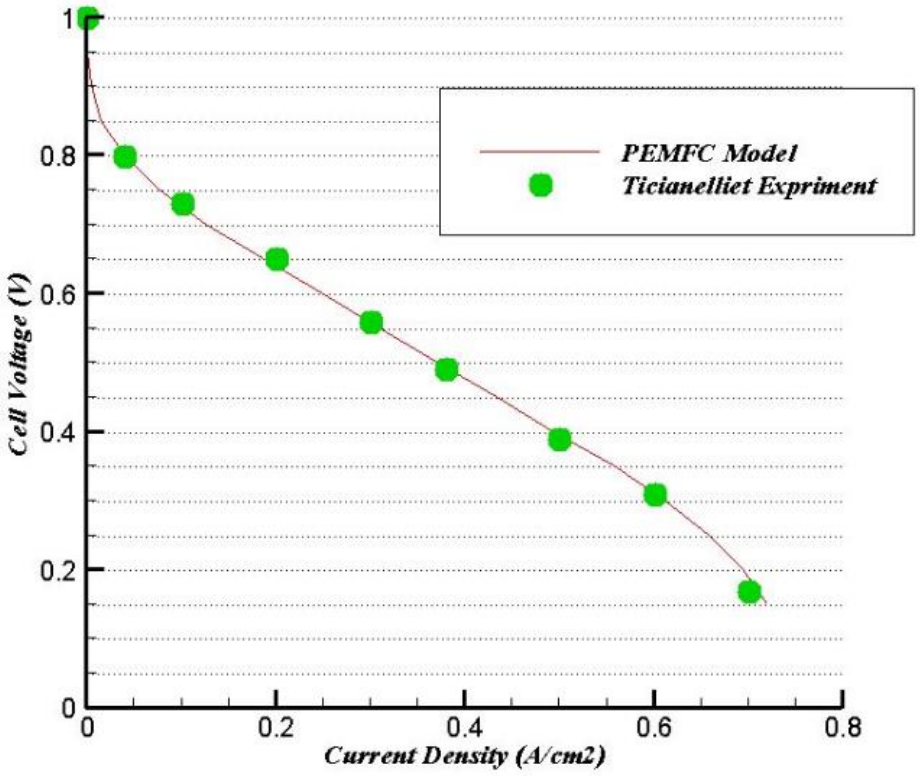

Figure 3. Validation of Polarization Curve of the presented model against that of Ticianelli's experimental work at T=323K and P=5atm

Velocity Profile

Figure4 shows the velocity vectors with their magnitudes in the channels. As it shows, velocity has its maximum value in the channel's center and due to no-slip condition it approaches to zero near the channel walls. Since the Darcy's source term has been applied to the momentum equations in the catalyst and gas diffusion layers, there are velocity vectors in these regions but at a very negligible order

of magnitude. As is depicted, velocity in the gas diffusion layer is a lot smaller than it is in the channel, the reason of which is a too thin backing layer (K = 1.76 ×(~10^{-7} cm^2).

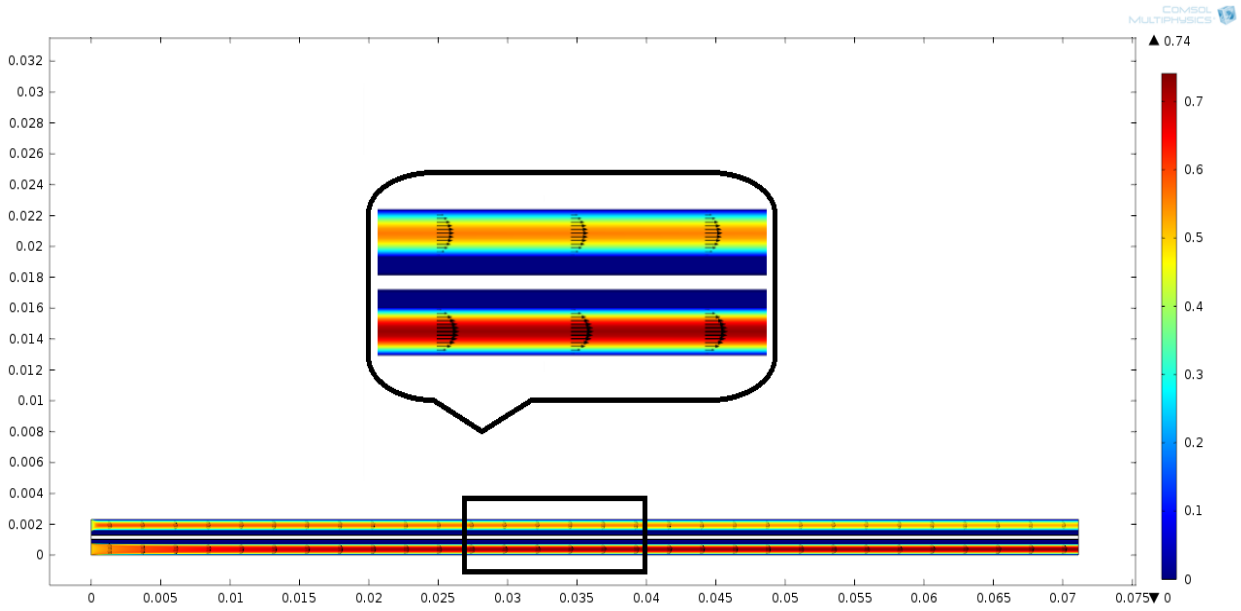

Figure4. Velocity Vector at 0.4V

Hydrogen mass fraction distribution

Figure 5 exhibits hydrogen mass fraction distribution. Since hydrogen is a reactant in anode and consumed in the anode catalyst layer, its mass fraction decreases along the cell length and also through the cell width from the channel to the anode catalyst layer. Hydrogen mass fraction is at its maximum extent at the channel inlet and at its minimum extent at the channel outlet in the catalyst layer. For the case of 0.4V these values are equal to 0.8 and 0.763, respectively. Moreover by comparing the minimum mass fraction at 0.4V and 0.6V, one can conclude that as the voltage increases, and as a result the current density decreases, Hydrogen mole fraction at outlet of the channel gets greater and the difference between fuel mole fraction at inlet and outlet will adopt a smaller value. It means that the less the voltage of the cell, the more the consumption of hydrogen will be.

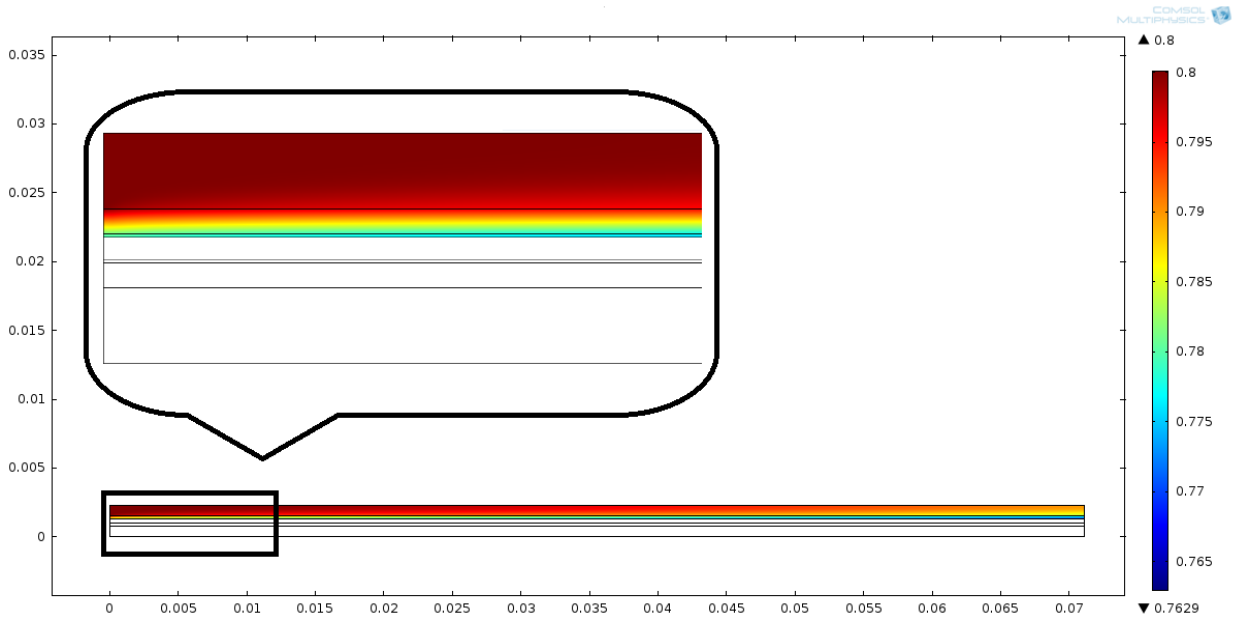

Figure 5. Hydrogen Mass Fraction at T=323K and V=0.4V

Oxygen mole fraction distribution

Figure 6 demonstrates the distribution of oxygen mole fraction at 0.4V. It can be seen in this figure that oxygen mole fraction decreases along the channel length. On the other hand, through the channel width, from air channel to catalyst layer, oxygen will not get to the consumption region (the interface between backing and catalyst layer) quickly, due to the weak diffusion in the backing layer. The maximum oxygen mole fraction occurs at the channel inlet and the minimum value occurs at the catalyst layer and channel outlet. These values are respectively 0.21 and 0.166 at 0.4V.

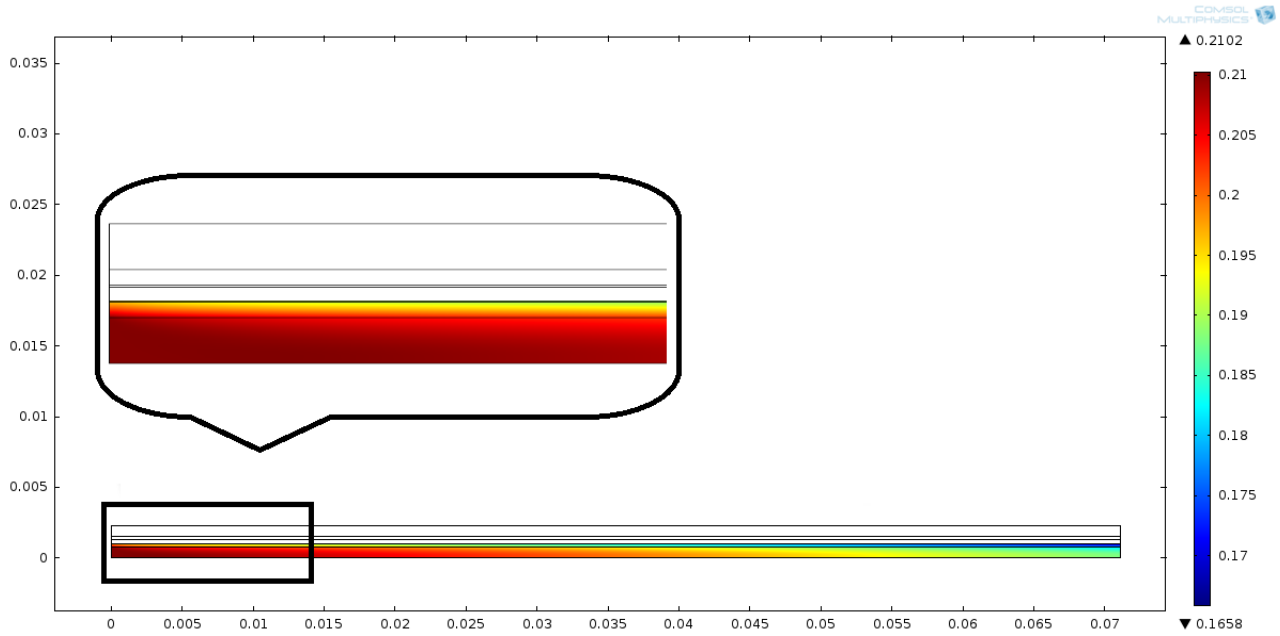

Figure 6. Oxygen Mole Fraction at T=323K and V=0.4V

Comparison of current densities and oxygen mole fractions at various voltages

Figure 7(a) and 7(b) show the current density and oxygen mole fraction at 0.4V, 0.6V and 0.8V. As is shown in these figures, current density decreases along the interface between backing layer and catalyst layer. This is due to oxygen consumption along the channel. Therefore the driving force needed to move oxygen towards the interface between the gas diffusion layer and the catalyst layer decreases. On the other hand by comparing these figures, it can be seen that the slopes of current density curve and oxygen mole fraction at higher currents (or lower V_{cell}) are more than those of low currents. This phenomenon is first of all, a result of more oxygen consumption in lower potentials, and then due to the effect of saturation.

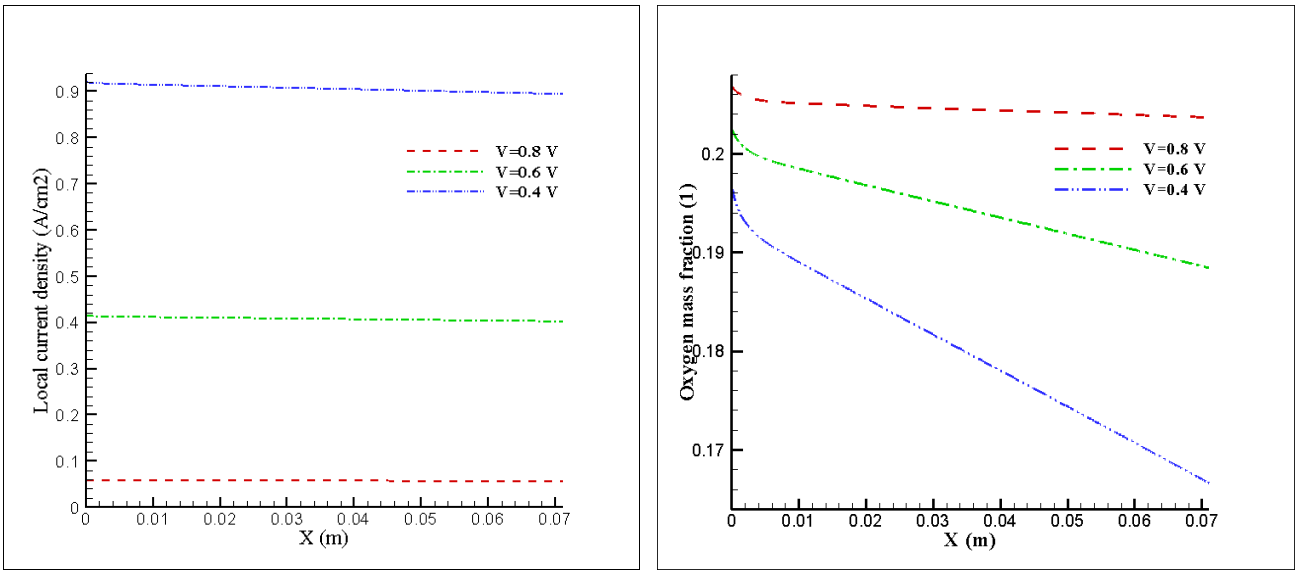

(a) Current density *(b)oxygen mole fraction*

Figure 7. Current Densities and Oxygen Mole Fractions

Along the Channel at V=0.4V, 0.6V and 0.8V

Saturation Level

Figure 8(a) and Figure 8(b) show the saturation level at 0.4V and 0.8V, respectively. As can be seen in this figure, the maximum value of saturation level occurs at the interface between the backing layer and the catalyst layer and is equal to 0.42 and its minimum value occurs at the cathode channel. This is due to the fact that electrochemical reactions happen at the catalyst surface. The produced water, which can't pass through the polymer electrolyte membrane, moves towards the backing layer. So the saturation level reaches to its highest level at the backing layer and the cathode catalyst layer.

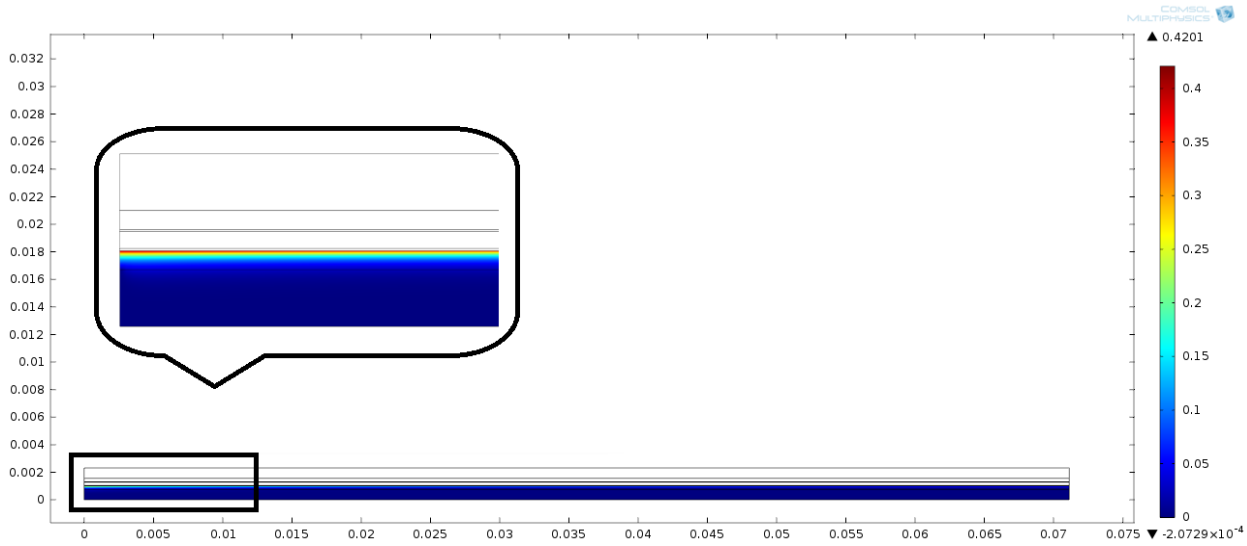

(a) Saturation level at 0.4V

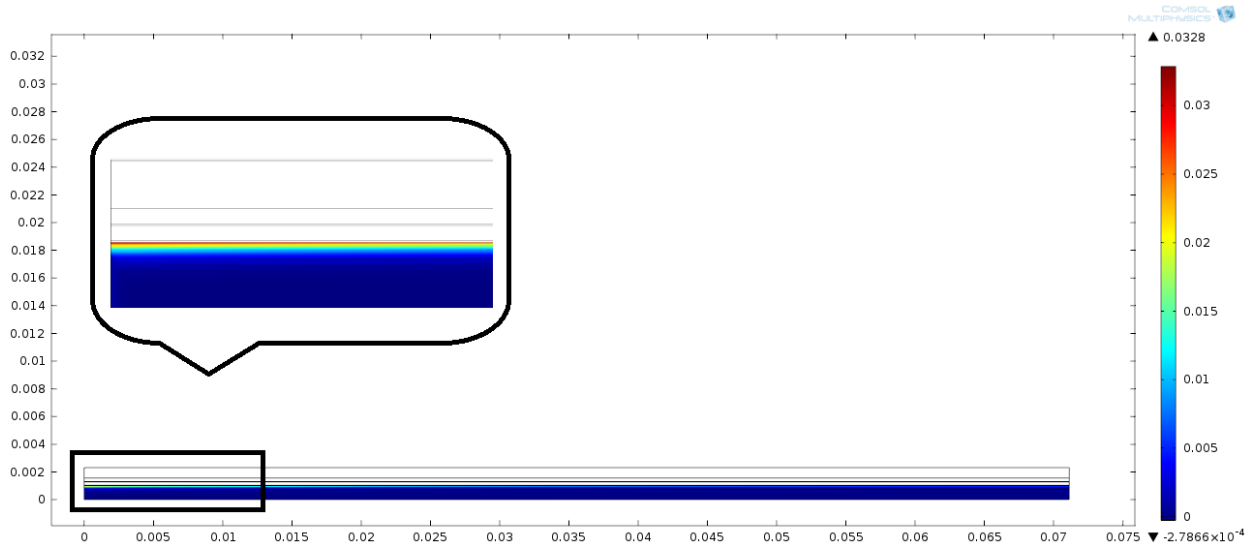

(b) Saturation level at 0.8V

Figure 8. Comparison of Saturation Level at 04V and 0.8V

4. Conclusion

In this study, the two-phase flow in a fuel cell has been simulated. In order to determine the saturation level at cathode, a separate mass conservation equation has been considered for liquid water at cathode. By determining the saturation level, other parameters that are related to the saturation level could be also determined consequently. By implementing these parameters in associated equations, different quantities of two-phase flow in the fuel cell were determined.

By solving conservation equations of mass and momentum, velocity contour was obtained and it was made clear that due to weak diffusion in the backing layer, the velocity value is insignificant. The conservation equation of chemical species determined the mass fractions of different species in the anode and cathode and it was shown that reactants are consumed along the cell and consequently their mass fractions would be decreased. On the other hand, water that is a product of the reaction is produced along the cell and its mass fraction is increased. Due to the production of water, oxygen's arrival to the reaction site is deferred and thus the current density decreases. Eventually, the saturation level at the cathode is depicted.

By studying different parameters of the model, these results have been clarified:

1. In polymer electrolyte membrane fuel cell at an operating temperature of 50°C, the critical current density is about 0.1 $A.cm^{-2}$. Thus in higher current densities two-phase flow is occurred in the fuel cell.
2. As the reactants' inlet velocity is increased, more water is produced. This happens because, as the velocity is increased, the driving force needed to drive the reactants to reaction site is increased and as a result, more current density will be produced. The increase in current density also results in more water production.
3. If pure oxygen is used at the inlet instead of air, water production is increased due to the increase of current density.
4. Formation of the two-phase region causes current density reduction and thus decreases in cell power.
5. As the humidity of the reactant gases increases, more water is produced.
6. By considering the current density distribution at catalyst layers, a more realistic model is obtained with respect to Khakbaz and Kermani's study.

References

1. Bernardi, D.M. and M.W. Verbrugge, *Mathematical model of a gas diffusion electrode bonded to a polymer electrolyte.* AIChE journal, 1991. **37**(8): p. 1151-1163.
2. Bernardi, D.M. and M.W. Verbrugge, *A mathematical model of the solid-polymer-electrolyte fuel cell.* Journal of the Electrochemical Society, 1992. **139**(9): p. 2477-2491.
3. Springer, T., M. Wilson, and S. Gottesfeld, *Modeling and experimental diagnostics in polymer electrolyte fuel cells.* Journal of the Electrochemical Society, 1993. **140**(12): p. 3513-3526.
4. Springer, T.E., T. Zawodzinski, and S. Gottesfeld, *Polymer electrolyte fuel cell model.* Journal of the Electrochemical Society, 1991. **138**(8): p. 2334-2342.
5. Fuller, T.F. and J. Newman, *Water and thermal management in solid-polymer-electrolyte fuel cells.* Journal of the Electrochemical Society, 1993. **140**(5): p. 1218-1225.
6. Nguyen, T.V. and R.E. White, *A water and heat management model for Proton-Exchange-Membrane fuel cells.* Journal of the Electrochemical Society, 1993. **140**(8): p. 2178-2186.
7. Gurau, V., H. Liu, and S. Kakac, *Two-dimensional model for proton exchange membrane fuel cells.* AIChE journal, 1998. **44**(11): p. 2410-2422.
8. Wang, Z., C. Wang, and K. Chen, *Two-phase flow and transport in the air cathode of proton exchange membrane fuel cells.* Journal of Power Sources, 2001. **94**(1): p. 40-50.
9. Khakbaz Baboli, M. and M. Kermani, *A two-dimensional, transient, compressible isothermal and two-phase model for the air-side electrode of PEM fuel cells.* Electrochimica Acta, 2008. **53**(26): p. 7644-7654.
10. Um, S., C.Y. Wang, and K. Chen, *Computational fluid dynamics modeling of proton exchange membrane fuel cells.* Journal of the Electrochemical Society, 2000. **147**(12): p. 4485-4493.
11. Wang, C., W. Gu, and B. Liaw, *Micro-Macroscopic Coupled Modeling of Batteries and Fuel Cells I. Model Development.* Journal of the Electrochemical Society, 1998. **145**(10): p. 3407-3417.
12. Baboli, M.K. and M. Kermani, *A two-dimensional, transient, compressible isothermal and two-phase model for the air-side electrode of PEM fuel cells.* Electrochimica Acta, 2008. **53**(26): p. 7644-7654.
13. Kermani, M. and J. Stockie†, *Heat and mass transfer modeling of dry gases in the cathode of PEM fuel cells.* International Journal of Computational Fluid Dynamics, 2004. **18**(2): p. 153-164.
14. Martin, J., P. Oshkai, and N. Djilali, *Flow structures in a U-shaped fuel cell flow channel: quantitative visualization using particle image velocimetry.* Journal of Fuel Cell Science and Technology, 2005. **2**(1): p. 70-80.
15. Ticianelli, E., et al., *Methods to advance technology of proton exchange membrane fuel cells.* Journal of the Electrochemical Society, 1988. **135**(9): p. 2209-2214.